



# Nanophytosome formulation of $\beta$ -1,3-glucan and *Euglena gracilis* extract for drug delivery applications<sup>☆</sup>



Varsha Virendra Palol<sup>a</sup>, Suresh Kumar Saravanan<sup>b</sup>, Sugunakar Vuree<sup>c</sup>,  
Raj Kumar Chinnadurai<sup>a</sup>, Veni Subramanyam<sup>a,\*</sup>

<sup>a</sup> Mahatma Gandhi Medical Advanced Research Institute (MGMRI), Sri Balaji Vidyapeeth (Deemed to-be University), Pillayarkuppam, Puducherry 607402, India

<sup>b</sup> Mahatma Gandhi Medical Preclinical Research Centre (MGMPRC), Sri Balaji Vidyapeeth (Deemed to-be University), Pillayarkuppam, Puducherry 607402, India

<sup>c</sup> MNR Foundation for Research and Innovation, MNR Medical College and Hospital, MNR Nagar, Fasalwadi, Narsapur Road, Sangareddy 502294, India

## ARTICLE INFO

### Method name:

Synthesis of Nanophytosomes

### Keywords:

Nanophytosome synthesis

Drug delivery

$\beta$ -1,3 glucan

*Euglena gracilis*

Solvent evaporation

Temperature

## ABSTRACT

*Euglena gracilis* (EG) is a unicellular freshwater alga known for its high  $\beta$ -1,3-glucan (BG) content with well-known biological properties and immune response. The high molecular weight structure of BG traditionally poses a challenge in terms of its size and absorption. Therefore, the aim of this study was to develop a novel drug delivery mechanism of BG and EG to nanophytosomes (NPs) by converting the heavy molecular weight of BG and EG into lipid phosphatidylcholine (PC), which plays an important role in improving their bioavailability and entrapment in captivity. The BG and EG NPs were developed by the solvent evaporation method while varying time and temperature to optimize their drug delivery ability. The size of BG-PC and EG-PC obtained by the Dynamic Light Scattering (DLS) method was 134.62 and 158.38 nm, respectively. Chemical (Fourier Transform Infra-Red) and structural (X-Ray Diffraction) characterization of NPs improved the binding capacity and the amorphous nature of both NPs. The shape of the NPs by Scanning electron microscopy (SEM) and Transmission electron microscopy (TEM) revealed their spherical, vesicular nature. The encapsulation efficiency of BG-PC and EG-PC was  $82 \pm 1.62\%$  and  $87 \pm 3.22\%$ , respectively, which improves the bioavailability. The developed methodology has thus proven effective in synthesizing BG-PC and EG-PC, which may be useful as NP drug delivery carriers. Future research could demonstrate the safety and effectiveness of long-term storage conditions for medical and pharmaceutical applications.

- Nanophytosomes are tailored in size, shape and composition to optimize the delivery of phytochemicals/phytocompounds through nanoscale size and surface modification for better physiological absorption.
- Nanophytosomes increase the stability of phytochemicals/phytocompounds and protect them from degradation due to heat or chemical reactions, leading to longer shelf life and improved therapeutic efficacy.
- In this method, optimal conditions were created for the formation of  $\beta$ -1,3-glucan and *Euglena gracilis* extract nanophytosomes for successful development of drug delivery system that can effectively deliver bioactive compounds.

<sup>☆</sup> **Related research article** W. Maryana, H. Rachmawati, D. Mudhakhir, Formation of phytosome containing silymarin using thin layer-hydration technique aimed for oral delivery, Mater. Today: Proc. 3(2016) 855-866. [10.1016/j.matpr.2016.02.019](https://doi.org/10.1016/j.matpr.2016.02.019)

\* Corresponding author.

E-mail addresses: [vsubramcidrf@gmail.com](mailto:vsubramcidrf@gmail.com), [venis@mgmari.sbvu.ac.in](mailto:venis@mgmari.sbvu.ac.in) (V. Subramanyam).

<https://doi.org/10.1016/j.mex.2023.102480>

Received 31 December 2022; Accepted 8 November 2023

Available online 20 November 2023

2215-0161/© 2023 The Author(s). Published by Elsevier B.V. This is an open access article under the CC BY-NC-ND license

(<http://creativecommons.org/licenses/by-nc-nd/4.0/>)

## Specifications table

Subject area:	Materials Science
More specific subject area:	Nanotechnology
Name of your method:	Synthesis of Nanophytosomes
Name and reference of original method:	Maryana, W.; Rachmawati, H.; Mudhakar, D. Formation of Phytosome Containing Silymarin Using Thin Layer-Hydration Technique Aimed for Oral Delivery. <i>Materials Today: Proceedings</i> , 3 (2016), 855–866 <a href="https://doi.org/10.1016/j.matpr.2016.02.019">10.1016/j.matpr.2016.02.019</a>
Resource availability:	The current method used in this manuscript was modified. Standard analytical, laboratory-grade chemicals and equipment were used. Equipment a) Rotary evaporator (Buchi – Rotavapour R-210) b) Lyophiliser (CHRIST- ALPHA 1-2 LD plus) c) Ultrasonicator (Sonic, Germany)  Chemicals/Reagents a) Phosphatidylcholine (PC) – Lipid (Sigma Aldrich) b) $\beta$ -1,3-glucan (Paramylon) – Pure (Sigma Aldrich) c) <i>Euglena gracilis</i> powder extract (CN Lab Nutrition, Asian group) d) Dimethylsulfoxide (Sigma Aldrich) e) Methanol (Sigma Aldrich) f) Chloroform (Sigma Aldrich)

## Method details

## Background

Nanophytosome (NP) technology is a kind of nanocarrier for drug delivery mechanisms to improve the bioavailability of phytochemical-derived nutraceuticals in food and pharmaceutical industries [1]. It is an herb/plant based vesicular delivery system that is more easily absorbed by the biological system than traditional extracts [2]. Traditional herbal medicines used for various medicinal purposes result in poor bioactivity, lipid solubility and incorrect molecular size, resulting in poor absorption and bioavailability. Therefore, a novel drug delivery system is in high demand compared to conventional herbal medicine, which paved the way for the emerging field of nanotechnology. As a rapidly evolving class of nanovesicles, NPs have received significant attention for phytochemical delivery [3]. The compatible molecular structures of NPs are formulated by incorporating the phytoactive compounds with phospholipids, especially phosphatidylcholine (PC). The structural composition of PC is similar to the cell membrane composition, which is later used as a potential vehicle in NP preparation due to its dual solubility and carrier properties. Some examples include quercetin phytosomes, which enhance the delivery of doxorubicin, a chemotherapy drug, to cells with increased permeability in the MCF-7 breast cancer cell line [4]. Silybin phytosome showed improved bioavailability when administered orally at 2,520 g daily in three divided doses to prostate cancer patients [5]. Likewise, the curcumin-phytosome complex was used as a complementary therapy for pancreatic cancer in the phase II study and proved that the active ingredient complex increased effectiveness [6]. Rutin NPs were developed to treat diabetic patients with high therapeutic efficiency and improve the bioavailability of rutin [7]. There are so many examples that show its therapeutic effect in several serious diseases.

Preparative steps play a crucial role in the development of novel drug delivery systems for therapeutic purposes, particularly in cancer treatment. On the other hand, size, average mean diameter and composition are essential characteristics and are modified for different applications, leading to numerous NP synthesis methods. Various methods such as solvent evaporation [8,9], thin film hydration [10], antisolvent precipitation method [11], co-solvent and salting out [12] have been used to prepare NPs.

In the current method, we used *Euglena gracilis* Z (EG), a unicellular photosynthesizing freshwater alga, which has a reserve of numerous vitamins and minerals with great industrial, commercial and biological applications [13]. EG consists of 80 % paramylon, an insoluble  $\beta$ -1,3-glucan (BG) [14], which is known for various medical applications in humans and improves immunological functions such as the treatment and prevention of infectious, oncological and viral diseases [15]. Aqueous extracts of EG exhibit potent antioxidant, pro- and anti-inflammatory innate responses and have been shown to be effective against lung carcinoma through apoptosis induction in mice [16,17]. Nevertheless, the high molecular weight of BG limits its ability to exert multiple anticancer mechanisms. Therefore, we described the synthesis of BG and EG-NP preparation in the current method by refluxing them with PC at a stoichiometric ratio (1:1) using a solvent evaporation method with different duration and temperature standardization. Measurement methods for nanomaterials are a rapidly growing topic, including effective physical and chemical characterization methods. It defines the type of connection through entrapment mechanisms and impurities on the surface of newly prepared NPs, which can be analyzed and characterized using various techniques. Therefore, in the current method article, we standardized BG and EG NPs by solvent evaporation technique and validated them for size and stability of NPs by dynamic light scattering (DLS), stability of NPs by zeta potential, chemical nature by Fourier transform infrared (FTIR), structure by X-ray diffraction (XRD), surface modification by scanning electron microscopy (SEM), and internal structure encapsulation by high-resolution transmission electron microscopy (HRTEM) techniques and encapsulation efficiency by means of UV-visible spectrophotometer. The aim of the study was to break down the high molecular weight of BG into smaller strands and incorporate them into PC to improve their encapsulation efficiency.

## Large scale synthesis of BG-PC

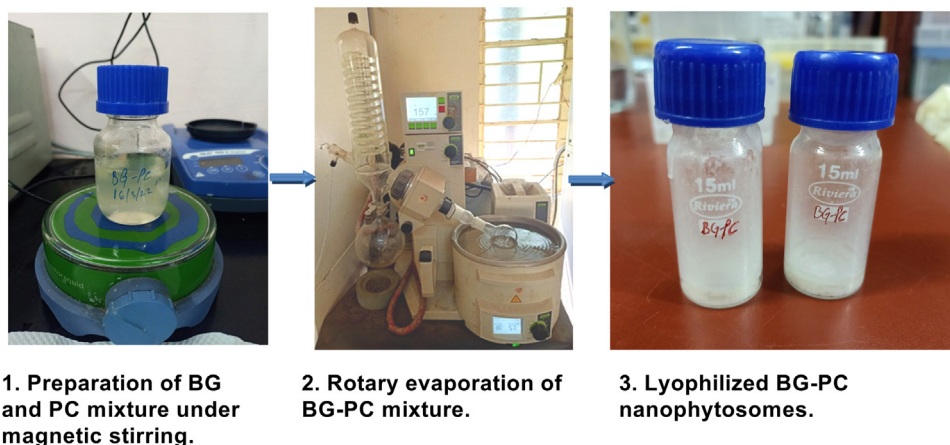


Fig. 1. A pictographic representation of the steps involved in synthesis of BG-PC nanophytosomes.

**Table 1**

Different heating temperatures and times for  $\beta$ -1,3-glucan nanophytosome (BG-PC) synthesis.

Temperature	BG heating (BG-PC1)	BG-PC heating (BG-PC2)
37 °C	4 h	4 h
60 °C	3 h	3 h
95 °C	2 h	2 h

Similarly, EG extract was also further developed into NP to ensure better bioavailability and stability. Given the potential advantages of BG and EG, the improved formulation of BG-PC and EG-PC may open new avenues in drug delivery systems.

### Novelty of the study

NPs are novel lipid vesicles designed to improve the delivery of herbal extracts. The novelty here is the application of NPs to encapsulate  $\beta$ -1,3-glucan (BG) and *Euglena gracilis* (EG) extract, potentially improving its bioavailability and efficacy of these natural ingredients. This is particularly relevant as traditional drug delivery systems may not be as efficient at delivering natural ingredients, insoluble large molecules such as the complex triple helix structure of BG. The study focuses on BG and EG extracts because BG has a complex triple helical structure that limits its bioavailability of poor solubility and BG is one of the vital components of EG. By breaking down the triple helix into single strands and incorporating them into PC, an NP-vesicular system is developed for drug delivery mechanisms in biological systems with various time and temperatures. The unique aspect lies in harnessing the potential of EG, a freshwater alga rich in BG (Paramylon) for biomedical applications. Previous research studies have focused less on the application of BG and EG in drug delivery systems for cancer treatment. Therefore, our study focuses on the development of potential BG and EG NPs for advanced drug carriers and shall have broader applications in pharmaceutical and biotechnological fields.

### Methodology for synthesis of nanophytosomes

#### Synthesis of $\beta$ -1,3-glucan derived nanophytosomes

##### Materials required

Phosphatidylcholine (PC): 6 mg/mL in chloroform  
 $\beta$ -1,3-glucan (BG): 4 mg/mL in DMSO

#### 1. Standardization of $\beta$ -1,3-glucan nanophytosomes

A 6 mg/mL stock solution of PC was prepared in chloroform and a 4 mg/mL stock solution of BG was dissolved in DMSO. The  $\beta$ -1,3-glucan nanophytosome (BG-PC) was developed in a ratio of 3:2 based on the weight of PC and BG. The triple helical nature of BG can be broken down into single strands by heating in a strong base like NaOH or solvents such as DMSO. Heating plays an important role in unwinding the triple helix into single strands, which helps in the preparation of nanomaterials to reduce the size of the molecule [18]. Therefore, two heating methods were used to resolve the triple helical nature of BG.

##### (A) BG-PC1 mixture preparation

The BG was heated for different durations and temperatures: 37 °C for 4 h, 60 °C for 3 h, and 95 °C for 2 h (Fig. 1, Table 1). After heating, the BG was added to PC in an Erlenmeyer flask (BG-PC1) in a volume ratio of 1:1 and stirred overnight.

### (B) BG-PC2 mixture preparation

The other method involved adding BG to PC at 1:1 ratio without heating BG, and the prepared BG-PC2 mixture was subjected to heating with different duration and temperature, 37 °C for 4 h, 60 °C for 3 h and 95 °C for 2 h. The different heating temperatures affect the concentration of the nanomaterial in mass to density and viscosity ratio, which mainly affects the size of the nanoparticles [19]. These two different heating methods explain how the dissolution of BG occurs and how it enhances the hydrogen bonding interaction with phospholipid (PC) to improve bioavailability. The pH was determined after heating the BG and BG-PC mixtures and was 7.0 for both heating methods. After stirring overnight, the solvent was evaporated using a nitrogen gas purge to ensure that any residual solvent remaining in the NP preparation was removed [20].

The BG-PCs obtained at different temperatures and times were analyzed by DLS for the size of the different BG-PCs obtained. Size was used as an initial parameter for standardization of NP synthesis.

## 2. Synthesis of BG-PC by Solvent evaporation method

### Procedure

- I. 6 mg/mL of PC stock solution was dissolved in chloroform.
- II. 4 mg/mL of BG was dissolved in DMSO and heated at 60 °C for 3 h.
- III. Both BG and PC were added to an Erlenmeyer flask in a ratio of given 1:1 for magnetic stirring at 350 rpm and synthesized overnight.
- IV. The prepared mixture was transferred to a 50 mL tube for ultrasonication.
- V. Ultrasonication was carried out for 5 min at 40 % amplitude and a pulse of 5 sec carried out under heat-free conditions by placing in ice.
- VI. BG-PC mixtures were concentrated for 3 h in a rotary evaporator at controlled temperatures and times. First, the mixture was concentrated at 60 °C for 1 h and then at 45 °C for 2 h [19].
- VII. The concentrated BG-PC mixture was stored at -80 °C for 4 h and lyophilized at a pressure of 40 mbar at -40 °C for 8 h to obtain BG-PC in powder form. The powdered BG-PC was stored at 4 °C for future experiments.

## 3. Synthesis of *Euglena gracilis* derived nanophytosomes

### Materials required

Phosphatidylcholine (PC): 1 mg/mL chloroform

*Euglena gracilis* extract (EG): 1 mg/mL methanol

The EG extract includes BG, wax esters, lipids and other vitamins and minerals, with the amount of BG in *Euglena* accounting for 40–60 % of the total weight. The *Euglena* NP (EG-PC) mixture was prepared in a 1:1 ratio. The EG extract was processed by centrifugation to remove residual contents of the extract.

### Procedure

#### Process of *Euglena* extract

- i. 20 mL methanol was used to dissolve 100 mg of *Euglena* extract powder.
- ii. The extract was centrifuged at 11,000 rpm for 30 min at 40 °C and the supernatant was collected.
- iii. 20 mL of fresh methanol was added to the pellet, stirred well and centrifuged as mentioned in step 2.
- iv. The second lot supernatant was found to be pale and the two supernatants were mixed and used for the synthesis of EG nanophytosomes.

#### *Euglena gracilis* Nanophytosome (EG-PC) synthesis

- i. 1 mg/mL PC stock solution was dissolved in chloroform.
- ii. EG extract and PC solution were added to the Erlenmeyer flask in a 1:1 ratio and stirred magnetically at 350 rpm overnight.
- iii. The EG-PC mixture was sonicated in a 50 mL tube for 5 min at 40 % amplitude and a 5 sec pulse in a beaker kept on ice.
- iv. The EG-PC mixture was concentrated in a rotary evaporator at 60 °C for 1 h, stored at -80 °C for 4 h, and lyophilized at a pressure of 40 mbar at -40 °C for 3 h to produce EG-PC in powder form. The powdered EG-PC was stored at 4 °C for future experiments (Fig. 2).

## 4. Characterisation of Nanophytosomes methodology

### (a) Dynamic Light scattering (DLS) and Zeta potential

The size of the NPs synthesized was measured by DLS on a Malvern NanoS (Malvern Instruments Ltd., UK) with light scattering at an angle of 173° at 25 °C. Zeta potential light scattering measurements were assessed on Beckman Coulter Delsa™ Nano, to determine the charge on the NPs, indicating stability. The NP mixture of BG-PC and EG-PC was diluted with water at a ratio of 1:10 as per the measurement requirements and was sonicated for 30 min. The NPs were filtered and the measurements were performed thrice.

## Large scale synthesis of EG-PC

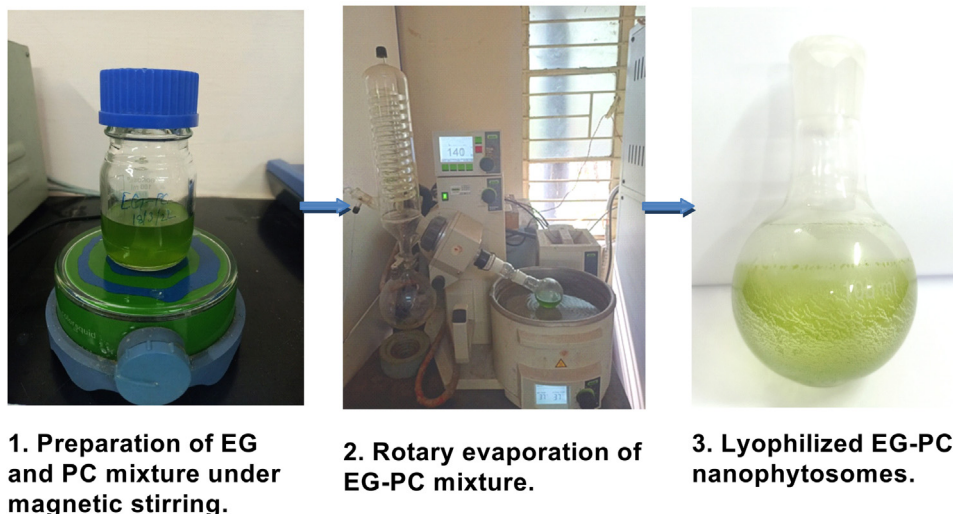


Fig. 2. A pictographic representation of the steps involved in synthesis of EG-PC nanophytosomes.

### (b) Fourier Transform Infra-red (FTIR)

FTIR was performed on the prepared NPs to determine the chemical groups. BG, EG, BG-NPs and EG-NPs were examined for the interaction of BG and EG with the PC compound. To determine the spectra of the compounds, the samples were mixed with potassium bromide (KBr) powder (1:1) in a mortar and pestle. The 4000–400  $\text{cm}^{-1}$  transmission spectral scan was used to characterize the NP of BG and EG.

### (c) X-Ray Diffraction (XRD)

The structural ion characterization of BG, EG, BG-NPs, and EG-NPs were carried out using an X-ray diffractometer (Bruker D8 Focus, Germany). The pattern was recorded using an X-ray machine equipped with a  $\text{Cu-K}\alpha$  radiation source. The experiment was carried out at room temperature according to the Bragg-Brentano geometry with a scattering range  $m(2\theta)$  of ranging from  $5^\circ$  to  $80^\circ$  at a scanning rate of  $0.02^\circ / \text{min}$ . The peaks were analyzed using origin Pro software.

### (d) Scanning electron microscopy (SEM)

The surface characterization of BG, EG, BG-NPs, and EG-NPs were visualized on SEM (VEGA3 TESCAN) at an accelerating voltage of 20 kV with magnifications ranging from 100 nm- 10  $\mu\text{m}$ . PC and BG were added to the grid in powder form, while a dilute suspension of EG, BG-PC and EG-PC was also added. After loading, the grids were air-dried. All samples underwent plasma sputtering (0.1 to 0.05 mbar) before viewing. The BG-PC and EG-PC NPs were analyzed using a FE-SEM (JEOL) at an accelerating voltage of 20kV and a magnification of 80,000X at a scale of 100 nm.

### (e) High-Resolution Transmission electron microscopy (HRTEM)

The NPs BG-PC and EG-PC were characterized using HRTEM (FEI Tecnai G2). The suspension of freshly produced NPs was diluted in ethanol at a ratio of 1:5 and sonicated for five min before the samples were tested. Before testing, the samples were laid out on a carbon-coated copper grid. The samples were then visualized in HRTEM at various magnifications in the range of 50–200 nm.

### 5. Encapsulation efficiency %

The amount of drug encapsulated/entrapped in the vesicle is indicated by the percent drug encapsulation. The encapsulated active ingredient (in the carrier) and the free active ingredient are separated as a first step in testing encapsulation effectiveness. The synthesized NPs prepared were measured spectrophotometrically before and after centrifugation. The centrifugation of NPs, BG-PC and EG-PC were done at 11,000 rpm at  $4^\circ\text{C}$  for 60 min. The supernatant containing free drug was measured spectrophotometrically at A290 nm. The percentage Encapsulation efficiency (%EE) was calculated using the formula

$$\frac{\% \text{ Encapsulation efficiency}}{(\%EE)} = \frac{W_{\text{Added drug}} - W_{\text{Free drug}}}{W_{\text{Added drug}}} \times 100$$

$W_{\text{Added drug}}$  is the amount of drug added during the preparation of NPs

$W_{\text{Free drug}}$  is the free drug obtained in the supernatant after centrifugation.

### Method validation

#### 1. (A) Particle size analysis of NPs by DLS

The size of the material is crucial for all prepared nanomaterials to enable the transport of the drugs to the desired target. The presence of PC in the NP helps to maintain structural stability and drug release in the correct ratio. The molecular weight of BG

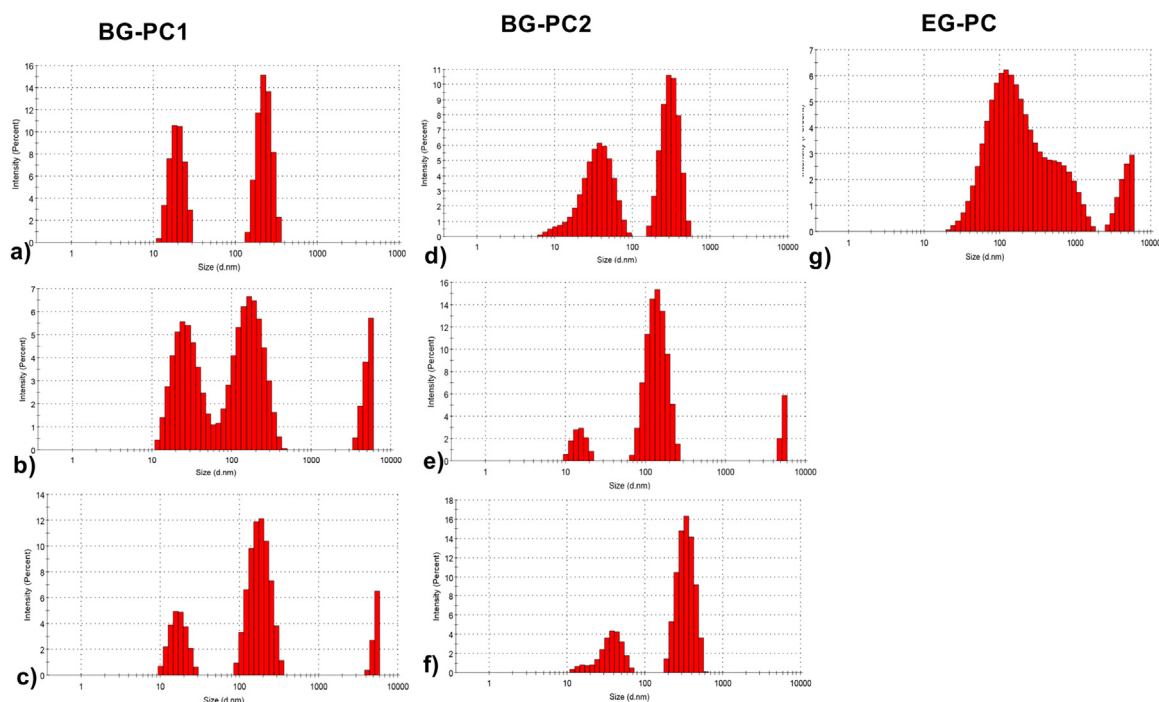


**Fig. 3.** Shows the size distribution of BG and EG-derived NPs. Fig. 3a), b) and c) represents only the heating of BG at 37 °C for 4 h; 60 °C for 3 h; 90 °C for 2 h of the prepared BG-PC NP. Fig. 3d), e) and f) represents heating the prepared BG-PC NP at 37 °C for 4 h; 60 °C for 3 h; 90 °C for 2 h without heating BG. Fig. 3g) represents EG-PC NP without heating.

**Table 2**  
Distribution of sizes of the prepared NPs at different temperatures.

	37°C	60°C	95°C
BG-PC1	234 nm	134.62 nm	190.96 nm
BG-PC2	386.69 nm	186.3 nm	301.71 nm
EG-PC	No heating		
	158.38 nm		

is about 500 kDa with a triple helical structure. To break them into individual strands, it was dissolved in DMSO and heated to different temperatures, making them fully soluble. Heating BG at different temperatures was performed to break down the triple helix structure into individual strands and preserve its active biological property [17]. The release of individual strands facilitates the synthesis of NP and helps in the efficient entrapment of the drug into PC. From Fig. 3a), the size of BG-PC1 where the BG was heated at 37 °C for 4 h was 234 nm, 3b) 60 °C for 3 h was 134.62 nm, 3c) 95 °C for 2 h, was 190.96 nm. This results in a broad size distribution in Fig. 3b) with an average size of less than 150 nm, which makes it optimal to carry out further experiments. From Fig. 3d), the size of BG-PC2 in which the prepared NP was heated at 37 °C for 4 h was 386.69 nm, in Fig. 3e) the size was heated at 60 °C for 3 h and was 186.3 nm, and in Fig. 3f) was heated at 95 °C for 2 h, 301.71 nm (Table 2). Thus, the optimal size of BG-PC was achieved at 60 °C for 3 h. It was notable that heating the NP mixture to high temperatures was not helpful in fabricating interactive active sites of PC. However, the BG heated to different temperatures shows an optimal size range with proven interactive active sites.

Fig. 3g) represents the EG-PC NP complex with the size 158.38 nm. EG was not heated because the essential component of EG is BG. Based on several studies on NP extracts, a standard temperature of 60 °C was used for the solvent evaporation technique and therefore no heating was used for EG-PC synthesis for initial standardization.

### (B) Stability of NPs by Zeta Potential

The zeta potential is an essential factor for the stability of colloidal dispersions. The charge of the NPs greater than  $\pm 30$  mV determines the stability of NPs in the phospholipid formulation [21]. From the DLS results, the obtained BG-PC and EG-PC NPs obtained were analyzed for zeta potential. The zeta potential of the prepared NPs BG-PC was 8.28 mV (Fig. 4a) and for EG-PC it was -30.38 mV (Fig. 4b). The values obtained show the colloidal stability of the prepared NPs. The BG structure has OH groups at the terminal group, which are likely to carry a negative charge when interacting with solvents. It is likely that PC carries both positively charged (choline) and negatively charged (phosphate and carbonyl) groups. Thus, when BG interacts with PC, the positive charge is preserved on the surface of BG-PC. The case of EG, which is composed of BG and a

## Zeta Potential

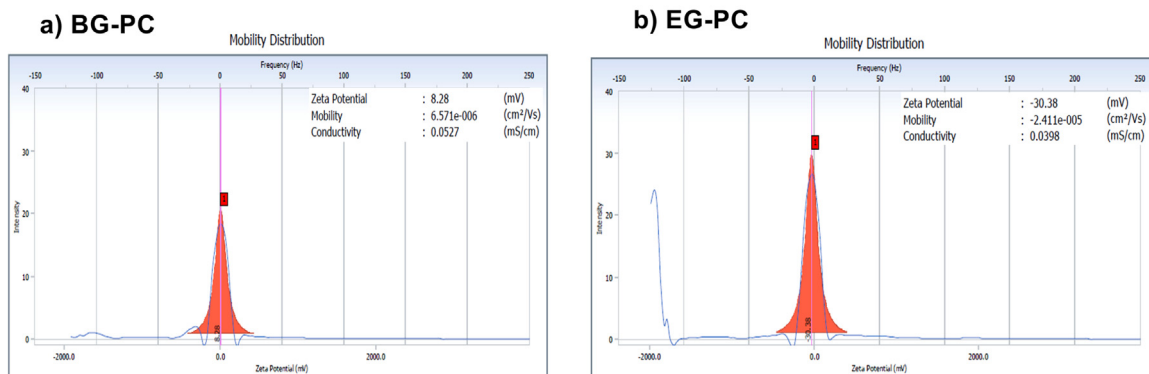


Fig. 4. Represents zeta potential of prepared NPs a) BG-PC b) EG-PC

mixture of wax esters, lipids and other components, produces a negative charge on the EG-PC surface when interacting with PC, describing the different interaction abilities of both NPs.

### 2. Fourier Transform Infra-red (FTIR)

The FTIR spectrum analysis was performed for PC, BG, BG-PC, EG, and EG-PC, as shown in Fig. 5. The PC shows characteristic peaks at  $3381.2\text{ cm}^{-1}$  (O-H band stretching),  $2925.1\text{ cm}^{-1}$  (choline group) and  $1234.5\text{ cm}^{-1}$  (phosphate head groups) [22], which are also found in NP- Structures of BG-PC were observed and EG-PC with changes in peak intensity, making them the characteristic feature of NP. The -OH stretching vibration is one of the essential areas for molecular interaction. The broader O-H peaks were observed in BG ( $3432.7\text{ cm}^{-1}$ ), representing the acidic group (-COO), while the similar peak was narrow in BG-PC, showing the O-H bonding interaction of BG with PC. This is possibly due to the high molecular weight of BG, which is released into individual strands upon heating and becomes more available for interaction with PC. At the same time, no difference in O-H bond stretch was observed in EG ( $3401.5\text{ cm}^{-1}$ ) and EG-PC ( $3387.6\text{ cm}^{-1}$ ).

The presence of the sugar group shows the characteristic feature of BG as it acts as a polysaccharide. The sugar ring group (C-O-C) in BG was found at a broader peak of  $1056.6\text{ cm}^{-1}$ , and the peak at  $888.8\text{ cm}^{-1}$  shows the absorption peak of -glycosidic bond. A similar peak with sharp intensity was observed in BG-PC at  $1077.7\text{ cm}^{-1}$ , and the absence of -glycosidic bond absorption in BG-PC contributed to further characteristic peaks at  $1461.2$  and  $1375.5\text{ cm}^{-1}$ , which attributed to the stretching vibration of -COO, C-C, and the symmetric stretching of C-H. A similar broader set of sugar groups was also found in EG at  $1053.1\text{ cm}^{-1}$ , confirming the presence of BGs in EG. Meanwhile, the similar intense peak in EG-PC at  $1069.6\text{ cm}^{-1}$  indicates the structural change of EG upon interaction with PC. The C-H stretching bands of the alkanes  $\text{CH}_3$  and  $\text{CH}_2$  lies between  $3000$  and  $2800\text{ cm}^{-1}$ . The band in PC ( $2925.1\text{ cm}^{-1}$ ) was clearly visible in BG-PC and EG-PC, while it was absent in BG and EG and had less intense peaks, indicating the interaction of the C-H bond in PC with BG and EC points out. The phosphate group ( $1234.5\text{ cm}^{-1}$ ) present in the polar head of PC was also found in BG-PC ( $1233.9\text{ cm}^{-1}$ ) and EG-PC ( $1234.9\text{ cm}^{-1}$ ) with lower intensity, indicating the interaction of the Phosphate bond with the explains surrounding molecules [23]. Thus, the peak variation observed at different wavelengths in BG-PC and EG-PC shows the characteristic feature of NP formation. The formation and change of additional peaks in BG-PC and EG-PC indicates the H-bonding and electrostatic interaction of BG and EG with PC.

### 3. X-ray diffraction (XRD)

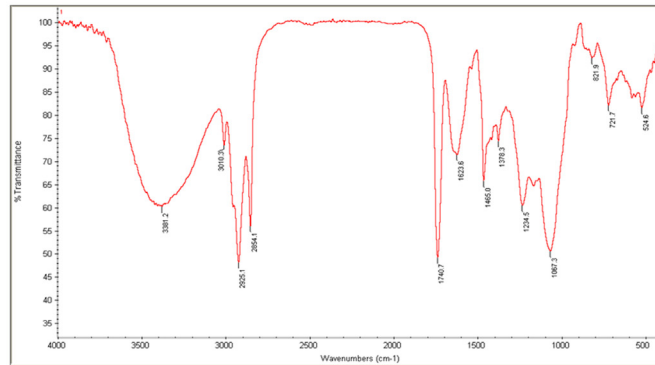
The addition of PC disrupts the crystallinity of BG, whereby a broad amorphous halo is observed between the two positions  $20.72^\circ$  and  $41.04^\circ$ . The loss of crystallinity is attributed to the dominance of choline and the other surfactants belonging to the phospholipid. The choline and surfactants bind easily to the BG (polysaccharide) and carbohydrate structures. Thus, the choline, the hydrophobic tail, inhibits the crystallization process, resulting in the amorphous form. Similarly, the XRD patterns obtained for EG-PC show the nature of the sample in an amorphous phase. From the diffraction pattern, it can be seen that the prepared samples retain the characteristic peaks of PC and EG, with the broad amorphous peak at position 2,  $19.27^\circ$ , and the small amorphous halo between positions 2,  $32.53^\circ$  and  $42.07^\circ$ . Since both PC and EG contain choline, surfactants, which belong to the phospholipids, form a homogeneous structure. The XRD spectrum correlates significantly with the FTIR analysis of the derived NPs compared to non-derived ones. The stacked diffraction patterns of the prepared NPs (BG-PC and EG-PC) only exhibit an amorphous nature (Fig. 6).

### 4. Surface structural analysis by Scanning Electron Microscopy (SEM)

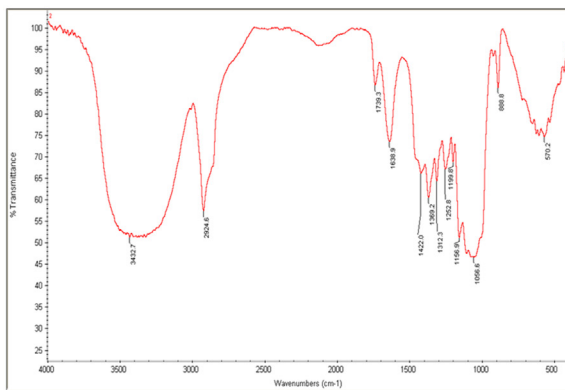
The surface morphology of NPs was analyzed by SEM. Fig. 7 illustrates the surface morphology of PC, which shows a big clump molecule aggregated due to its sticky nature; meanwhile, BG shows a distinct rod-like structure, whereas BG-PC forms a spherical molecule. In the case of EG, the extract shows small, round-like bodies, while EG-PC shows protruding spherical vesicles. Field emission SEM (FESEM) analysis was also performed on NPs BG-PC (Fig. 7f) and EG-PC (Fig. 7g), which shows the magnified image of NPs at 80,000X magnification with even distribution in spherical shape at the range of 100nm. The

## Fourier Transform Infra-Red

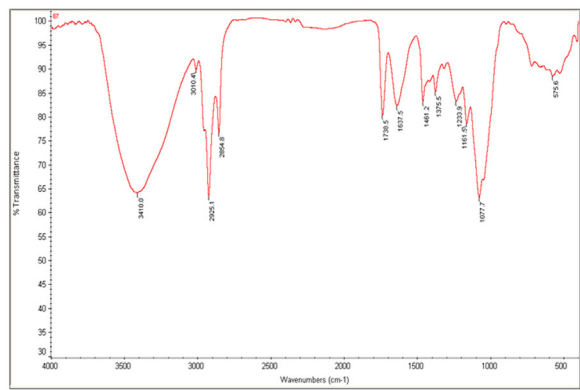
a) PC



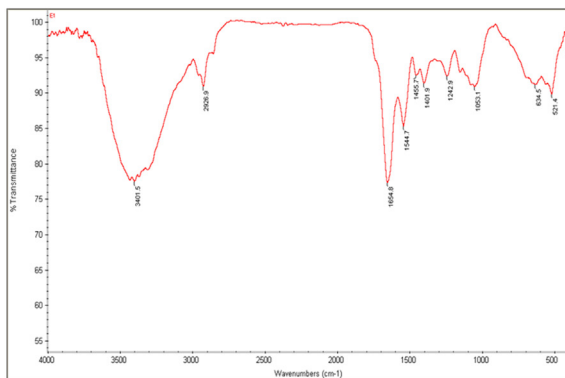
b) BG



c) BG-PC



d) EG



e) EG-PC

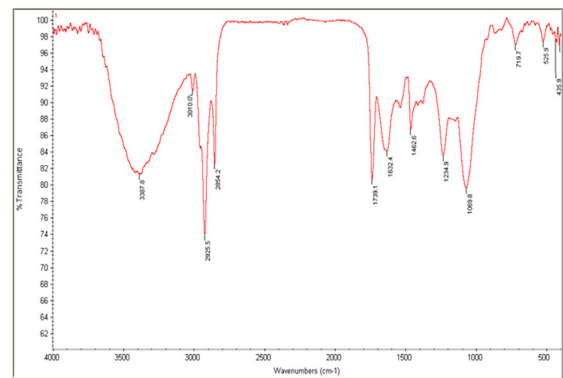


**Fig. 5.** Represents FTIR spectra peaks of a) Phosphatidylcholine (PC) – Lipid, b)  $\beta$ -1,3 glucan (BG)- Polysaccharide, c)  $\beta$ -1,3 glucan nanophytosome (BG-PC), d) *Euglena gracilis* extract (EG) e) *Euglena gracilis* extract nanophytosome (EG-PC).

above analysis shows how the incorporation of PC played an essential role in changing the morphology of both BG-PC and EG-PC, which signifies the shape and synthesis of NPs.

### 5. Inner structural analysis of NPs by HRTEM

The HRTEM analysis was performed to investigate the internal morphology, shape and size of the obtained NPs. Upon collision, the PCs exhibit a lumpy texture (Fig. 8a). In contrast, BG-PC shows distinct spherical-shaped NPs at 200 and 100 nm (Fig. 8b). Similarly, EG-PC formed several small spherical-shaped NPs at 200 and 100 nm (Fig. 8c). It was found that few of them collided



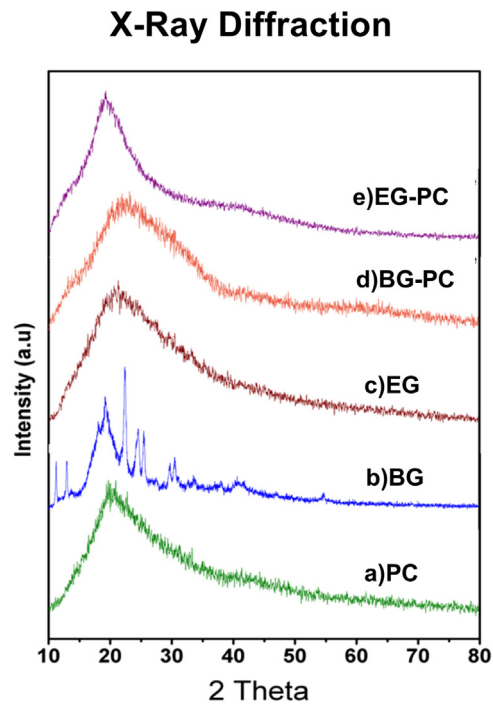


**Fig. 6.** Comparison of X-ray diffraction peaks of a) Phosphatidylcholine (PC), b)  $\beta$ -1,3 glucan (BG), c) *Euglena gracilis* extract (EG), d)  $\beta$ -1,3 glucan nanophytosome (BG-PC) and e) *Euglena gracilis* nanophytosome (EG-PC).

### Scanning electron Microscopy

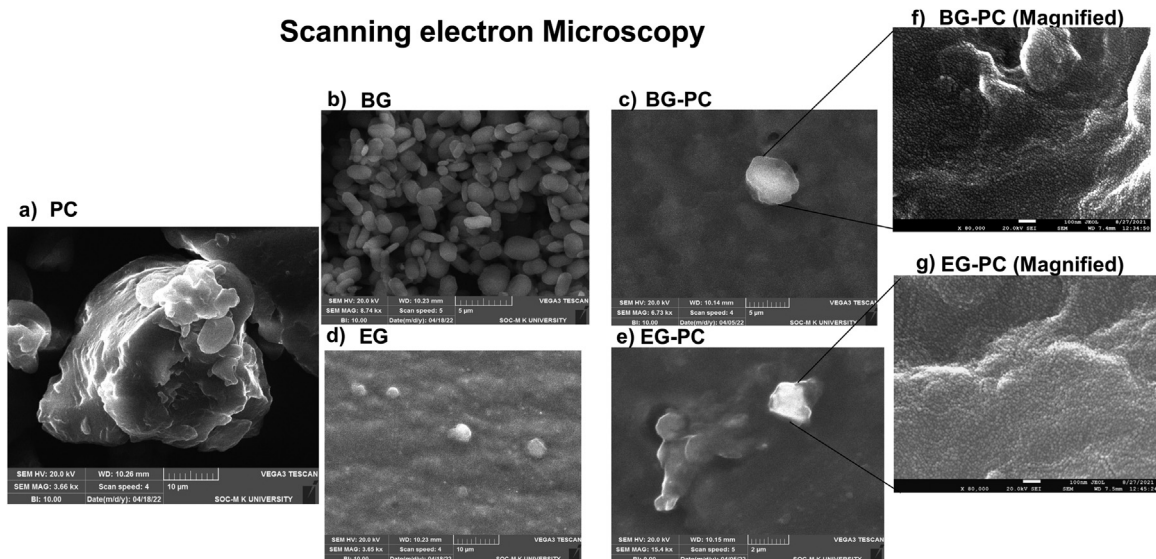


**Fig. 7.** presents scanning electron microscope (SEM) images of a) phosphatidylcholine (PC) - lipid, b)  $\beta$ -1,3 glucan (BG) - pure compound, c)  $\beta$ -1,3 glucan nanophytosome (BG-PC), d) *Euglena gracilis* extract (EG), and e) *Euglena gracilis* nanophytosome (EG-PC) at different scales of 2.5 and 10  $\mu$ m. f) and g) represents the enlarged image of BG-PC and EG-PC, respectively, with a magnification of 80,000X and a scale of 100 nm, with uniformly distributed spherical NPs with a statistic of  $n = 3$ .

with each other, which might be due to wide distribution of NPs and formation of aggregates. Thus, BG-PC was found to have a more distinct in shape than EG-PC.

#### 6. Encapsulation efficiency (EE) of NPs

The encapsulation/entrapment efficiency of NPs depends on drug solubility and bonding interaction of PC, which leads to matrix formation. The higher EE % is used as a significant parameter to evaluate the success of drug delivery systems. In this study, BG-PC and EG-PC showed EE % as  $82 \pm 1.62$  % and  $87 \pm 3.22$  % respectively. The EE % of the developed NPs offer higher

## Transmission electron Microscopy

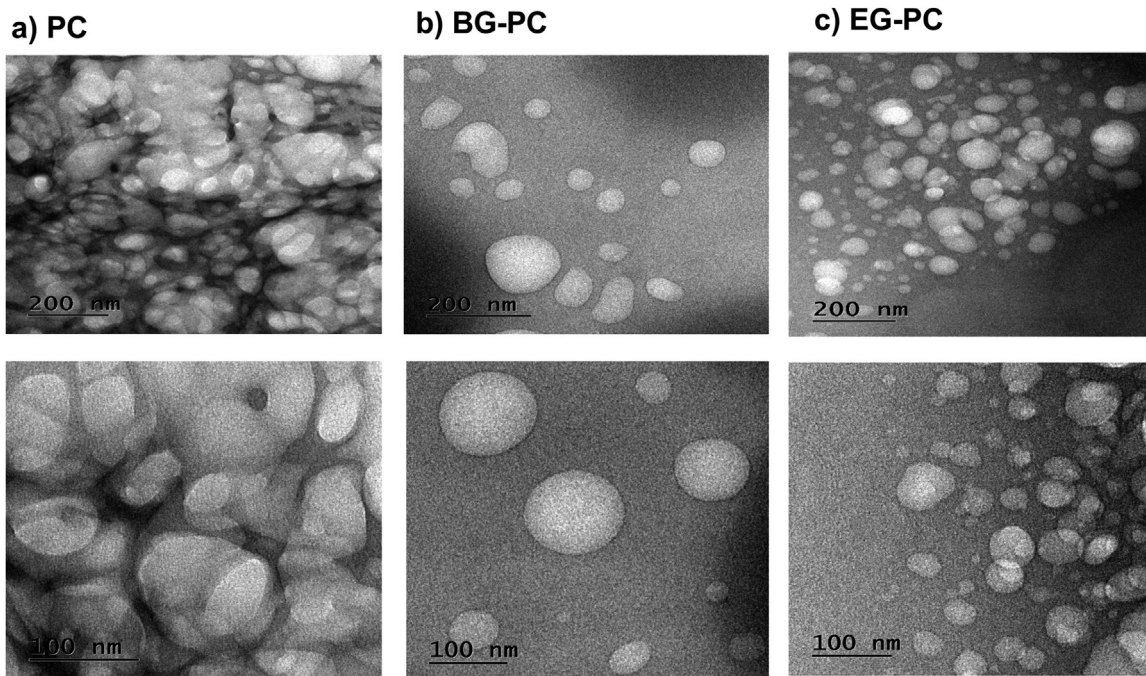


**Fig. 8.** Presents high resolution transmission electron microscopy (HRTEM) images of a) Phosphatidylcholine (PC) - lipid, b)  $\beta$ -1,3 glucan nanophytosome (BG-PC), c) *Euglena gracilis* nanophytosome (EG-PC) at various scales of 200 and 100 nm with  $n = 3$ .

encapsulation of both NPs; however, EG-PC showed higher EE % than BG-PC. A higher EE % also showed better bioavailability of the prepared NPs, which could deliver its potential efficiency when incorporated into biological systems [24].

### Discussion

Phytochemicals have come a long way over the years in exhibiting tremendous potential in several diseases. However, there are a few constraints which limit their ability to completely explore its biological activity. The use of nanocarrier has been very essential in addressing these drawbacks by developing different forms of these compounds into a carrier molecule which supports their structure, stability, absorption, solubility and bioavailability. One among them is, nanophytosomes which is a lipid carrier drug delivery mechanism by embedding the phytoconstituents into the head of the phospholipid such as phosphatidylcholine [25]. Standardization plays a significant role in obtaining the optimum size and surface morphology to define drug delivery mechanisms. According to recorded case studies, the methodologies used to measure nanoparticles based on their size, shape, chemical composition, thermal conductivity, etc., have emerged as powerful analytical techniques defining nanomaterials' nature. The standardization will ensure the quality and development of next-generation nanomaterials for applications in several diseases like cancer and gene therapies [26]. Studies have also reported the efficacy and safety of using lipid-based nanoformulations in developing SARS-CoV-2 vaccines [27,28].

In the current study, algal extracts of EG and its major component BG was developed into NPs as they have potential health benefits. The optimization of developing these NPs was performed using solvent evaporation method with varying durations and temperatures. From which, 60 °C for 3 h was found to be optimum for BG-PC with size of 134.62 nm, while for EG-PC it was optimum without heating at the size of 158.38 nm. The achieved size by DLS was the critical initial factor for optimization, as size plays a major role in developing NPs. The zeta potential activity showed the BG-PC and EG-PC to be 8.28 and -30.38 mV respectively, which was found to enhance the stability of the obtained NPs. The chemical profile and interactions of BG-PC and EG-PC were compared to that of PC, BG and EG which exhibited distinct changes in the peak exhibiting various intermolecular interactions. The structural analysis of NPs by XRD exhibited the change of crystalline BG to amorphous BG-PC and significant peak changes in EG-PC also contributed to the NP formation. The size and surface chemistry are essential for synthesizing nanomaterials for drug absorption bioavailability, and the nano-size range is efficient in crossing permeability barriers [29]. The surface morphology analysis by SEM and FE-SEM revealed changes in the BG-PC and EG-PC structure when compared to the non-derived ones. The FE-SEM showed small, spherical arranged NPs with even distribution. The TEM analysis helps in understanding the internal environment and drug entrapment to the PC in developing the matrix [30]. The BG-PC and EG-PC exhibited spherical distinct vesicles at scale of 100 nm. The entrapment efficiency of the NPs, BG-PC and EG-PC were found to be  $82 \pm 1.62$  and  $87 \pm 3.22$  % respectively which is considered optimum for

enhancing bioavailability [31]. With all optimization the NPs represent prominent physical and chemical characterizations, however, few limitations of the study include analyzing the *in vitro* drug release profile of NPs which is essential to study the release profile over time duration which plays pivotal role in biological system. Studies have reported issues with stability of NPs over long term storage which could affect its efficacy and toxicity [26,32].

Phytosomes are viewed as highly effective nano-sized carriers for delivering substances, but transitioning from product development to successful commercialization is a complex journey [33]. Despite their numerous benefits, only a few phytosomal products have made it to the market. Once formulated effectively, one major hurdle in bringing NPs to market is ensuring their safety. Fortunately, NPs have structurally neutral properties, making their introduction into the human body generally safe without concerns about adverse reactions or immunological responses [34]. However, given their small size, it's essential to assess various factors like bioaccumulation, biocompatibility, metabolism, and excretion before marketing them [35]. Large-scale production of NPs presents another challenge. During scaling up, it's crucial to maintain the product's characteristics, especially for pH-sensitive NPs, which have low physicochemical stability, posing challenges in industrial production [3]. Phytosome formulations should undergo long-term stability testing under various storage conditions to ensure their viability and efficacy over time. Accelerated stability testing can help predict the shelf life of the product with strict limitations [36]. However, with their increased popularity over the years due to their biocompatibility, affordability, and safety, which has added to their rapid commercialization and manufacturing process, several pharmaceuticals industries have also explored the advantages and biocompatibility of these NP formulations.

Thus, in this study, the BG- and EG- NPs optimization helped in minimizing changes in vesicle size, and aggregation by preserving the integrity of the encapsulated NPs. The NPs prepared with an integral part of the membrane anchoring the molecules through chemical bonds to the polar head of the phospholipid will serve as an advanced delivery system to produce desired molecular complex with improved absorption and bioavailability of phytoconstituents in *Euglena gracilis* and further research on exploring its biological activities can be of potential benefit in several diseases including cancer.

## Conclusion

In the current study, the solvent evaporation technique was used to investigate the effect of formulation variables of  $\beta$ -1,3-glucan and *Euglena gracilis* extract on the physicochemical properties of the synthesized NPs. Thin-film hydration and lyophilization techniques were successfully used to prepare the NPs, and their size and surface properties were systematically optimized. We characterized the optimized NP formulation using nanoscale ISO limits of PDI, enhanced surface charge, amorphous nature, simplified structure, and reasonable entrapment efficiency without losing the effective composition. The researchers found that phospholipids were essential for improving the absorption, bioavailability and solubility of phytochemicals in NPs with poorly soluble phytochemicals, which was found to be evident from our study. In this work, the relevance of using lipids in the production of NP, a nano-based medical formulation, was highlighted. Nevertheless, further research is needed to confirm the use of drug delivery in biological systems with long-term stability of viability and efficacy over time.

## Declaration of Competing Interest

The authors declare that they have no known competing financial interests or personal relationships that could have appeared to influence the work reported in this paper.

## CRedit authorship contribution statement

**Varsha Virendra Palol:** Conceptualization, Methodology, Data curation, Writing – original draft. **Suresh Kumar Saravanan:** Writing – review & editing. **Sugunakar Vuree:** Data curation, Writing – review & editing. **Raj Kumar Chinnadurai:** Writing – review & editing. **Veni Subramanyam:** Conceptualization, Project administration, Supervision, Data curation, Writing – review & editing.

## Data availability

Data will be made available on request.

## Ethics statements

Not applicable

## Acknowledgments

- The authors would like to acknowledge Sri Balaji Vidyapeeth (Deemed to-be University) for providing the M.V.K Iyer fellowship.
- The authors would like to acknowledge Dr. Kumaresan G, Dept. of Genetics, Madurai Kamaraj University, for providing UGC-NRCBS Visiting fellow, equipment and lab support.
- The authors would like to acknowledge Dr. Ratnakar Arumugam, School of Biomedical sciences, Sri Balaji Vidyapeeth (Deemed to-be University) for helping in interpretation of XRD analysis.

- The authors would like to acknowledge the Central Instrumentation facility of Pondicherry University for providing DLS and FTIR support.
- The authors would like to acknowledge the Central Instrumentation facility of the Indian Institute of Science Education and Research (IISER) Bhopal for providing Zeta Potential instrument support.
- The authors would like to acknowledge the Central Instrumentation facility of Lovely Professional University for providing FE-SEM support.
- The authors would like to acknowledge the Central Instrumentation facility of Madurai Kamaraj University for providing SEM and HRTEM support.

## References

- [1] A. Babazadeh, S.M. Jafari, B. Shi, Chapter Ten - encapsulation of food ingredients by nanophytosomes. In *Lipid-Based Nanostructures for Food Encapsulation Purposes*, in: Nanoencapsulation in the Food Industry, Academic Press, Australia, 2019, pp. 405–443, doi:10.1016/B978-0-12-815673-5.00010-6.
- [2] M.A. Saleemi, V. Lim, Phytosomes used for herbal drug delivery, in: *Pharmaceutical Nanobiotechnology for Targeted Therapy*, Springer International Publishing, Cham, 2022, pp. 255–279, doi:10.1007/978-3-031-12658-1\_9.
- [3] M. Barani, E. Sangiovanni, M. Angarano, M.A. Rajizadeh, M. Mehrabani, S. Piazza, H.V. Gangadharappa, A. Pardakhty, M. Mehrbani, M. Dell'Agli, M.H. Neamatollahi, Phytosomes as innovative delivery systems for phytochemicals: A comprehensive review of literature, *Int. J. Nanomed.* 16 (2021) 6983–7022, doi:10.2147/IJN.S318416.
- [4] A. Minaei, M. Sabzichi, F. Ramezani, H. Hamishehkar, N. Samadi, Co-delivery with nano-quercetin enhances doxorubicin-mediated cytotoxicity against MCF-7 cells, *Mol. Biol. Rep.* 43 (2) (2016) 99–105, doi:10.1007/s11033-016-3942-x.
- [5] T.W. Flaig, D.L. Gustafson, L.J. Su, J.A. Zirrolli, F. Crighton, G.S. Harrison, A.S. Pierson, R. Agarwal, L.M. Glodé, A phase I and pharmacokinetic study of silybin-phytosome in prostate cancer patients, *Investig. New Drugs* 25 (2) (2007) 139–146, doi:10.1007/s10637-006-9019-2.
- [6] D. Pastorelli, A.S.C. Fabricio, P. Giovanis, S. D'Ippolito, P. Fiduccia, C. Soldà, A. Buda, C. Sperti, R. Bardini, G. Da Dalt, G. Rainato, M. Gion, F. Ursini, Phytosome complex of curcumin as complementary therapy of advanced pancreatic cancer improves safety and efficacy of gemcitabine: results of a prospective phase II trial, *Pharmacol. Res.* 132 (2018) 72–79, doi:10.1016/j.phrs.2018.03.013.
- [7] S. Amjadi, F. Shahnaz, B. Shokouhi, Y. Azarmi, M. Siah-Shadbad, S. Ghanbarzadeh, M. Kouhsoltani, A. Ebrahimi, H. Hamishehkar, Nanophytosomes for enhancement of rutin efficacy in oral administration for diabetes treatment in streptozotocin-induced diabetic rats, *Int. J. Pharm.* 610 (2021) 121208, doi:10.1016/j.ijpharm.2021.121208.
- [8] L. Zou, F. Chen, J. Bao, S. Wang, L. Wang, M. Chen, C. He, Y. Wang, Preparation, characterization, and anticancer efficacy of evodiamine-loaded PLGA nanoparticles, *Drug Deliv.* 23 (3) (2016) 908–916, doi:10.3109/10717544.2014.920936.
- [9] F. Yu, Y. Li, Q. Chen, Y. He, H. Wang, L. Yang, S. Guo, Z. Meng, J. Cui, M. Xue, X.D. Chen, Monodisperse microparticles loaded with the self-assembled berberine-phospholipid complex-based phytosomes for improving oral bioavailability and enhancing hypoglycemic efficiency, *Eur. J. Pharm. Biopharm.* 103 (2016) 136–148, doi:10.1016/j.ejpb.2016.03.019.
- [10] S. Nandhini, K. Ilango, Development and characterization of a nano-drug delivery system containing vasaka phospholipid complex to improve bioavailability using quality by design approach, *Res. Pharm. Sci.* 16 (1) (2021) 103, doi:10.4103/1735-5362.305193.
- [11] R.P. Singh, R. Narke, Preparation and evaluation of phytosome of lawsone, *Int. J. Pharm. Sci. Res.* 6 (12) (2015) 5217–5226, doi:10.13040/IJPSR.0975-8232.6(12).5217-26.
- [12] S.F. El-Menshawy, A.A. Ali, M.A. Rabeh, N.M. Khalil, Nanosized soy phytosome-based thermogel as topical anti-obesity formulation: an approach for acceptable level of evidence of an effective novel herbal weight loss product, *Int. J. Nanomed.* 13 (2018) 307–318, doi:10.2147/IJN.S153429.
- [13] A. Gissibl, A. Sun, A. Care, H. Nevalainen, A. Sunna, Bioproducts from *Euglena Gracilis*: synthesis and applications, *Front. Bioeng. Biotechnol.* 7 (2019) 108, doi:10.3389/fbioe.2019.00108.
- [14] Y. Wang, T. Seppänen-Laakso, H. Rischer, M.G. Wiebe, *Euglena Gracilis* growth and cell composition under different temperature, light and trophic conditions, *PLoS One* 13 (4) (2018) e0195329, doi:10.1371/journal.pone.0195329.
- [15] T. Watanabe, R. Shimada, A. Matsuyama, M. Yuasa, H. Sawamura, E. Yoshida, K. Suzuki, Antitumor activity of the  $\beta$ -glucan paramylon from *Euglena* against preneoplastic colon aberrant crypt foci in mice, *Food Funct.* 4 (11) (2013) 1685–1690, doi:10.1039/c3fo60256g.
- [16] S. Ishiguro, D. Upreti, N. Robben, R. Burghart, M. Loyd, D. Ogun, T. Le, J. Delzeit, A. Nakashima, R. Thakkar, A. Nakashima, K. Suzuki, J. Comer, M. Tamura, Water extract from *Euglena Gracilis* prevents lung carcinoma growth in mice by attenuation of the myeloid-derived cell population, *Biomed. Pharmacother.* 127 (2020) 110166, doi:10.1016/j.biopha.2020.110166.
- [17] F.C. Phillips, G.S. Jensen, L. Showman, R. Tonda, G. Horst, R. Levine, Particulate and solubilized  $\beta$ -glucan and non- $\beta$ -glucan fractions of *Euglena gracilis* induce pro- and anti-inflammatory innate immune cell responses and exhibit antioxidant properties, *J. Inflamm. Res.* 12 (2019) 49–64, doi:10.2147/JIR.S191824.
- [18] J. Hwang, K. Lee, A.A. Gilad, J. Choi, Synthesis of beta-glucan nanoparticles for the delivery of single strand DNA, *Biotechnol. Bioproc. E* 23 (2) (2018) 144–149, doi:10.1007/s12257-018-0003-4.
- [19] N.A. Shah, I.L. Animasau, J.D. Chung, A. Wakif, F.I. Alao, C.S.K. Raju, Significance of nanoparticle's radius, heat flux due to concentration gradient, and mass flux due to temperature gradient: the case of water conveying copper nanoparticles, *Sci. Rep.* 11 (1) (2021) 1882, doi:10.1038/s41598-021-81417-y.
- [20] M.S. Freag, Y.S. Elnaggar, O.Y. Abdallah, Lyophilized phytosomal nanocarriers as platforms for enhanced diosmin delivery: optimization and *ex vivo* permeation, *Int. J. Nanomed.* 8 (2013) 2385–2397, doi:10.2147/IJN.S45231.
- [21] R.G. Shriram, A. Moin, H.F. Alotaibi, E.S. Khafagy, A. Al Saqr, A.S. Abu Lila, R.N. Charyulu, Phytosomes as a plausible nano-delivery system for enhanced oral bioavailability and improved hepatoprotective activity of silymarin, *Pharmaceuticals* 15 (7) (2022) 790 (Basel), doi:10.3390/ph15070790.
- [22] T. Aissaoui, Novel contribution to the chemical structure of choline chloride based deep eutectic solvents, *Pharm. Anal. Acta* 6 (11) (2015) 448.
- [23] W. Pohle, D.R. Gauger, H. Fritzsche, B. Rattay, C. Selle, H. Binder, H. Böhlh, FTIR-spectroscopic characterization of phosphocholine-headgroup model compounds, *J. Mol. Struct.* 563–564 (2001) 463–467, doi:10.1016/S0022-2860(00)00830-9.
- [24] P. Pal, V. Dave, S. Paliwal, M. Sharma, M.B. Potdar, A. Tyagi, Phytosomes—Nanoarchitectures' promising clinical applications and therapeutics, in: *Nanopharmaceutical Advanced Delivery Systems*, John Wiley & Sons, Ltd, India, 2021, pp. 187–216, doi:10.1002/9781119711698.ch9.
- [25] S.S. Gaikwad, Y.V. Morade, A.M. Kothule, S.J. Kshirsagar, U.D. Laddha, K.S. Salunkhe, Overview of phytosomes in treating cancer: advancement, challenges, and future outlook, *Heliyon* 9 (6) (2023) e16561, doi:10.1016/j.heliyon.2023.e16561.
- [26] S.Z. Alshawwa, A.A. Kassem, R.M. Farid, S.K. Mostafa, G.S. Labib, Nanocarrier drug delivery systems: characterization, limitations, future perspectives and implementation of artificial intelligence, *Pharmaceutics* 14 (4) (2022) 883, doi:10.3390/pharmaceutics14040883.
- [27] Y. Takechi-Haraya, T. Ohgita, Y. Demizu, H. Saito, K. Izutsu, K. Sakai-Kato, Current status and challenges of analytical methods for evaluation of size and surface modification of nanoparticle-based drug formulations, *AAPS PharmSciTech* 23 (5) (2022) 150, doi:10.1208/s12249-022-02303-y.
- [28] X. Hou, T. Zaks, R. Langer, Y. Dong, Lipid nanoparticles for mRNA delivery, *Nat. Rev. Mater.* 6 (12) (2021) 1078–1094, doi:10.1038/s41578-021-00358-0.
- [29] A. Banerjee, J. Qi, R. Gogoi, J. Wong, S. Mitragotri, Role of nanoparticle size, shape and surface chemistry in oral drug delivery, *J. Control Release* 238 (2016) 176–185, doi:10.1016/j.jconrel.2016.07.051.
- [30] S. Tripathy, D.K. Patel, L. Barob, S.K. Naira, A Review on phytosomes, their characterization, advancement & potential for transdermal application, *J. Drug Deliv. Ther.* 3 (3) (2013) 147–152, doi:10.22270/jddt.v3i3.508.
- [31] D.A. Gaber, M.A. Alnawis, N.L. Alotaibi, R.A. Almutairi, S.S. Alsaed, S.A. Abdoun, A.M. Alsubaiyel, Design and optimization of ganciclovir solid dispersion for improving its bioavailability, *Drug Deliv.* 29 (1) (2022) 1836–1847, doi:10.1080/10717544.2022.2083723.
- [32] N. Desai, Challenges in development of nanoparticle-based therapeutics, *AAPS J.* 14 (2) (2012) 282–295, doi:10.1208/s12248-012-9339-4.

- [33] A.D. Permana, R.N. Utami, A.J. Courtenay, M.A. Manggau, R.F. Donnelly, L. Rahman, Phytosomal nanocarriers as platforms for improved delivery of natural antioxidant and photoprotective compounds in propolis: an approach for enhanced both dissolution behaviour in biorelevant media and skin retention profiles, *J. Photochem. Photobiol. B* 205 (2020) 111846, doi:[10.1016/j.jphotobiol.2020.111846](https://doi.org/10.1016/j.jphotobiol.2020.111846).
- [34] A. Babazadeh, M. Zeinali, H. Hamishehkar, Nano-phytosome: a developing platform for herbal anti-cancer agents in cancer therapy, *Curr. Drug Targets* 19 (2) (2018) 170–180, doi:[10.2174/1389450118666170508095250](https://doi.org/10.2174/1389450118666170508095250).
- [35] I.P. Kaur, V. Kakkar, P.K. Deol, M. Yadav, M. Singh, I. Sharma, Issues and concerns in nanotech product development and its commercialization, *J. Control Release* 193 (2014) 51–62, doi:[10.1016/j.jconrel.2014.06.005](https://doi.org/10.1016/j.jconrel.2014.06.005).
- [36] A. Evers, D. Clénet, S. Pfeiffer-Marek, Long-term stability prediction for developability assessment of biopharmaceutics using advanced kinetic modeling, *Pharmaceutics* 14 (2) (2022) 375, doi:[10.3390/pharmaceutics14020375](https://doi.org/10.3390/pharmaceutics14020375).